Available online at www.sciencedirect.com

ScienceDirect

Journal of Molecular Structure 797 (2006) 99–110

Journal of MOLECULAR STRUCTURE

www.elsevier.com/locate/molstruc

Monensin A benzyl ester and its complexes with monovalent metal cations studied by spectroscopic, mass spectrometry and semiempirical methods

Adam Huczyński [a], Dominik Michalak [a], Piotr Przybylski [a], Bogumil Brzezinski [a,*], Franz Bartl [b]

[a] *Faculty of Chemistry, A. Mickiewicz University, Grunwaldzka 6, 60-780 Poznan, Poland*
[b] *Institute of Medical Physics and Biophysics Charité – Universitätsmedizin Berlin Campus Charité Mitte, Ziegelstr. 5/9, 10117 Berlin, Germany*

Received 10 February 2006; accepted 1 March 2006
Available online 24 April 2006

Abstract

Monensin A benzyl ester (MON3) was synthesized and its ability to form complexes with Li^+, Na^+ and K^+ cations was studied by ESI MS, ^1H and ^{13}C NMR, FT-IR and PM5 semiempirical methods. MON3 has been found to preferentially form complex with Na^+ cations. The formation of stable complexes of 1:1 stoichiometry up to $cv = 70$ V is indicated in the electrospray ionisation mass spectra. With increasing cone voltage value, the fragmentation of the respective complexes is detected and is connected primary with the dehydration process. The structures of the complexes are stabilized by intramolecular hydrogen bonds in which the OH groups are always involved. The structures of MON3 and its complexes with Li^+, Na^+ and K^+ cations are visualized and discussed in detail. It is shown that in the structure of MON3 the oxygen atom of this C=O ester group is involved in very weak bifurcated hydrogen bonds with two hydroxyl groups. Within the complexes of MON3 with Li^+ and K^+ cations, this C=O ester group is not hydrogen bonded, whereas in the structure of MON3 with Na^+ it can also coordinate this cation. Such a structure is, however, not dominant in acetonitrile solution. It is demonstrated that the formation of a pseudo-crown ring structure formed by MON3 prefers the complexation of Na^+ cations.

Keywords: Monensin A; Benzyl ester; Complexes; Monovalent cations; ^1H NMR; ^{13}C NMR; HETCOR; COSY; FT-IR; ESI mass spectrometry; PM5 calculations; Hydrogen bonds

1. Introduction

Monensin A is one of the most important polyether antibiotic ionophores employed as a veterinary drug. It is used as a growth-promoting agent and as a coccidiostat in beef cattle, sheep, chickens, and turkeys [1–5]. Monensin readily forms lipid-soluble pseudo-macrocyclic complexes with mono- and divalent cations [6–14] and regulates many cellular functions, including apoptosis. It causes the collapse of sodium and potassium gradients at the plasma membrane, blocks intracellular protein transport, and exhibits antibiotic, antimalarial, and other important biological activities [15–24]. The reason why monensin exhibits various pharmacological and biological activities is its ability to disrupt the Na^+/K^+ ion balance across the cell membranes, which finally leads to the cell death.

Recently, we have studied the nature of complexes between monensin A methyl ester and monovalent as well as divalent cations, by various spectroscopic, mass spectrometry and semiempirical methods. This ester has been shown to have especially high affinity to Na^+ and Ca^{2+} cations [25,26]. As a continuation of these studies we report here ESI MS, ^1H and ^{13}C NMR, FT-IR as well as PM5 studies of the complexation

---

[*] Corresponding author. Tel.: +48 61 829 1330; fax: +48 61 865 8008.
E-mail address: bbrzez@main.amu.edu.pl (B. Brzezinski).

0022-2860/$ - see front matter © 2006 Elsevier B.V. All rights reserved.
doi:10.1016/j.molstruc.2006.03.014

ability of benzyl ester of Monensin A with monovalent cations such as the Li^+, Na^+ and K^+ cations. The structures of the Monensin A benzyl ester and its complexes with monovalent cations are discussed in detail.

2. Experimental

Monensin A sodium salt was purchased from Sigma (90–95%). The perchlorates $LiClO_4$, $NaClO_4$ and $KClO_4$ were commercial products of Sigma and were used without any further purification. Because the salts were hydrates, it was necessary to dehydrate them at several (6–10 times) evaporation steps from a 1:5 mixture of acetonitrile and absolute ethanol. The dehydration of the perchlorates was followed by recording of their FT-IR spectra in acetonitrile.

CD_3CN and CH_3CN spectral-grade solvents were stored over 3 Å molecular sieves for several days. All manipulations with the substances were performed in a carefully dried and CO_2-free glove box.

2.1. Synthesis of monensin benzyl ester (MON3)

Monensin A sodium salt was dissolved in dichloromethane and stirred vigorously with a layer of aqueous sulphuric acid (pH 1.5). The organic layer containing MONA was washed with distilled water, and dichloromethane was evaporated under reduced pressure to dryness.

A mixture of benzyl bromide (250 mg, 1.45 mmol), MONA (500 mg, 0.75 mmol), and 1,8-diazacicyclo[5.4.0] undec-7-en (DBU) (175 mg, 1.15 mmol) and 40 ml toluene was heated at 90 °C for 5 h. After cooling, the precipitate DBU-hydrobromide (DBU · HBr) was filtered and washed hexane. The filtrate and the washing were combined and were evaporated under reduced pressure. The residue was purified by chromatography on silica gel (Fluka type 60) to give MON3 (510 mg, 89% yield) as a colourless oil showing a tendency to form a glass state. Elementary analysis: Calculated: C, 67.87%; H, 9.01%. Found: C, 67.85%; H, 9.04%.

2.2. Synthesis of MON3 complexes with monovalent cations

The 0.07 mol L^{-1} solutions of 1:1 complexes of MON3 with monovalent cations (Li^+, Na^+ and K^+) were obtained by adding equimolar amounts of $MClO_4$ salt (M = Li, Na, K) dissolved in acetonitrile to MON3 dissolved in acetonitrile. The solvent was evaporated under reduced pressure to dryness and the oily residue was dissolved in an appropriate volume of dry CH_3CN or CD_3CN.

2.3. Mass spectrometry

The electrospray ionisation (ESI) mass spectra were recorded on a Waters/Micromass (Manchester, UK) ZQ mass spectrometer equipped with a Harvard Apparatus syringe pump. All samples were prepared in acetonitrile. The measurements were performed for the two types of

Table 1
The main peaks in the ESI mass spectra of the complexes of MON3 with cations at various cone voltages

Cation	Cone voltage (V)	Main peaks *m/z*
Li^+	10	768
	30	768
	50	768
	70	768
	90	768, 750
	110	768, 750, 732, 485, 467, 445, 427
	130	768, 750, 732, 485,467, 445, 427
Na^+	10	784
	30	784
	50	784
	70	784
	90	784
	110	784, 766
	130	784, 766, 748, 507, 501, 489, 483, 479, 461, 443
K^+	10	800
	30	800
	50	800
	70	800
	90	800, 782, 764
	110	800, 782, 764
	130	800, 782, 764

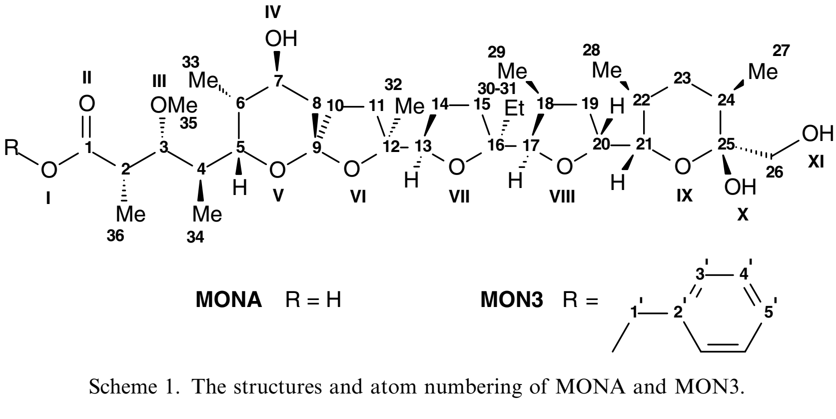

Scheme 1. The structures and atom numbering of MONA and MON3.

samples being the solutions of MON3 (5×10^{-5} mol L^{-1}) with: (a) each of the cations Li^+, Na^+ and K^+ (2.5×10^{-4} mol L^{-1}) taken separately and (b) the cations Li^+, Na^+ and K^+ ($5 \times 10^{-5}/3$ mol L^{-1}) taken together. The samples were infused into the ESI source using a Harvard pump at a flow rate of 20 μl min^{-1}. The ESI

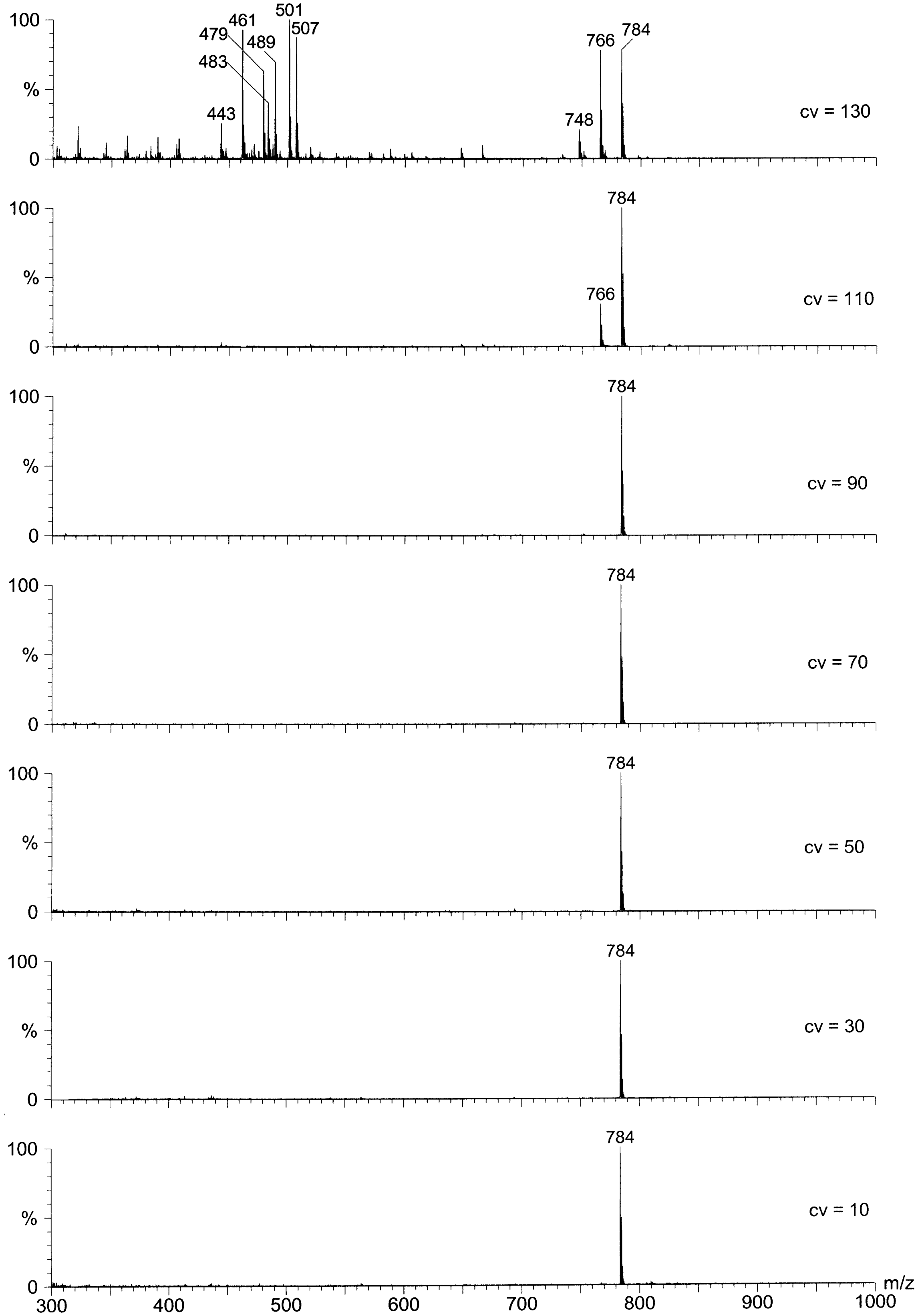

Fig. 1. ESI mass spectra of a 1:1 mixture of MON3 with Na^+ at various cone voltages (cv).

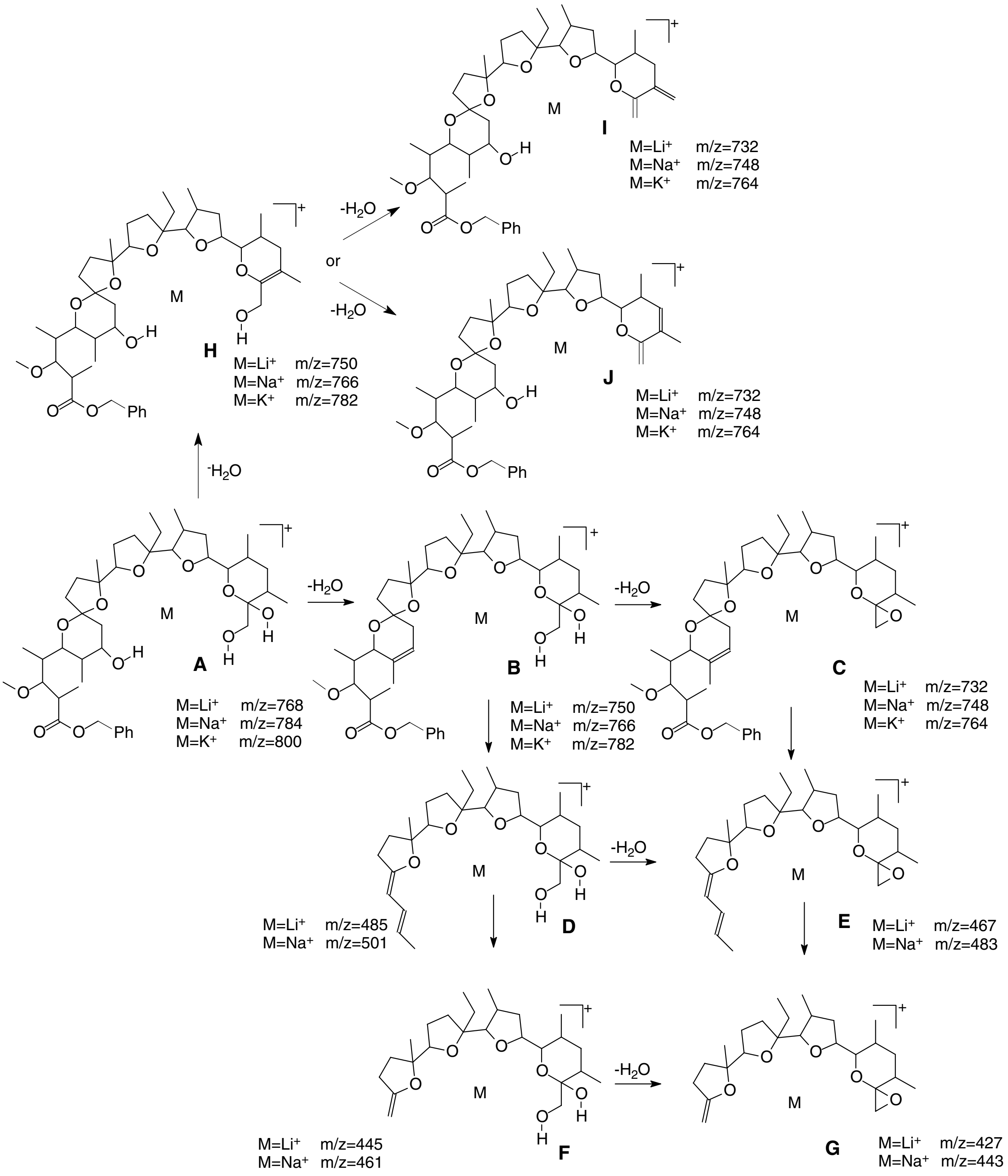

Scheme 2. The proposed fragmentation pathways of MON3 complexes with monovalent cations.

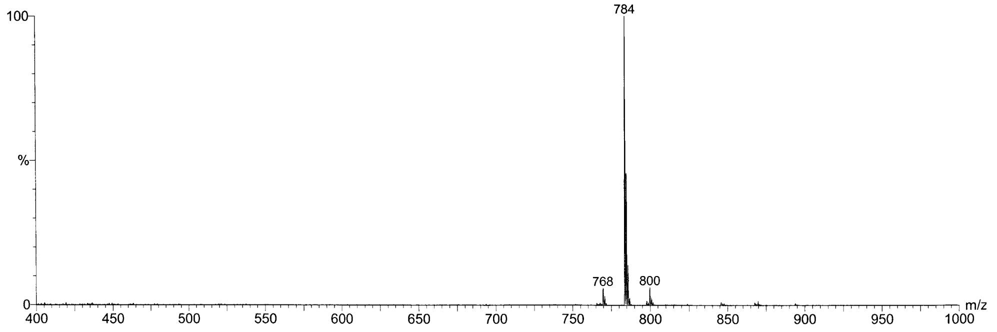

Fig. 2. ESI mass spectrum of a 1:1:1:3 mixture of cation perchlorates $LiClO_4$, $NaClO_4$ and $KClO_4$ and MON3 (cv = 30).

source potentials were: capillary 3 kV, lens 0.5 kV, extractor 4 V. The standard ESI mass spectra were recorded at the cone voltages 10, 30, 50, 70, 90, 110 and 130 V. The source temperature was 120 °C and the dessolvation temperature was 300 °C. Nitrogen was used as the nebulizing and dessolvation gas at flow rates of 100 and 300 L h^{-1}, respectively. Mass spectra were acquired in the positive ion detection mode with unit mass resolution at step size of 1 m/z unit. The mass range for ESI experiments was from $m/z = 300$ to $m/z = 1000$.

Table 2
^1H NMR chemical shifts (ppm) of MON3 and its complexes in CD_3CN

No. atom	Chemical shift (ppm)				Differences (Δ) between chemical shifts (ppm)		
	MON3	MON3:Li^+	MON3:Na^+	MON3:K^+	Δ1	Δ2	Δ3
1	–	–	–	–	–	–	–
2	2.68	2.67	2.73	2.70	−0.01	0.05	0.02
3	3.55	3.60	3.57	3.56	0.05	0.02	0.01
4	1.98	1.99	2.01	1.92	0.01	0.03	−0.06
5	4.04	4.16	3.95	3.98	0.12	−0.09	−0.06
6	1.74	1.69	1.67	1.68	−0.05	−0.07	−0.06
7	3.66	3.96	3.87	3.76	0.30	0.21	0.10
8A	1.62	1.56	1.62	1.64	−0.06	0.00	0.02
8B	1.99	2.05	2.01	1.99	0.06	0.02	0.00
9	–	–	–	–	–	–	–
10A	1.87	1.85	1.79	1.76	−0.02	−0.08	−0.11
10B	1.93	2.05	2.00	1.86	0.12	0.07	−0.07
11A	1.72	1.85	1.82	1.80	0.13	0.10	0.08
11B	1.92	1.89	1.90	1.86	−0.03	−0.02	−0.06
12	–	–	–	–	–	–	–
13	3.64	3.67	3.62	3.54	0.03	−0.02	−0.10
14A	1.57	1.42	1.46	1.46	−0.15	−0.11	−0.11
14B	1.76	1.89	1.89	1.76	0.13	0.13	0.00
15A	1.58	1.52	1.45	1.48	−0.06	−0.13	−0.10
15B	2.08	2.16	2.25	2.18	0.08	0.17	0.10
16	–	–	–	–	–	–	–
17	3.86	4.37	3.95	3.93	0.51	0.09	0.07
18	2.27	2.43	2.31	2.33	0.16	0.04	0.06
19A	1.48	1.55	1.63	1.50	0.07	0.15	0.02
19B	2.15	2.33	2.15	2.19	0.18	0.00	0.04
20	4.19	4.40	4.41	4.34	0.21	0.22	0.15
21	3.59	3.81	3.72	3.65	0.22	0.13	0.06
22	1.33	1.39	1.49	1.33	0.06	0.16	0.00
23A	1.24	1.35	1.32	1.31	0.11	0.08	0.07
23B	1.41	1.52	1.46	1.46	0.11	0.05	0.05
24	1.69	1.90	1.68	1.68	0.21	−0.01	−0.01
25	–	–	–	–	–	–	–
26A	3.33	3.43	3.46	3.39	0.10	0.13	0.06
26B	3.33	3.45	3.65	3.56	0.12	0.32	0.23
27	0.81	0.83	0.80	0.80	0.02	−0.01	−0.01
28	0.86	0.82	0.83	0.85	−0.04	−0.03	−0.01
29	0.94	0.95	0.90	0.93	0.01	−0.04	−0.01
30A	1.55	1.54	1.48	1.50	−0.01	−0.07	−0.05
30B	1.55	1.70	1.72	1.65	0.15	0.17	0.10
31	0.90	0.96	0.90	0.91	0.06	0.00	0.01
32	1.30	1.54	1.45	1.41	0.24	0.15	0.11
33	0.86	0.88	0.86	0.86	0.02	0.00	0.00
34	0.96	0.96	0.98	0.95	0.00	0.02	−0.01
35	3.23	3.21	3.23	3.23	−0.02	0.00	0.00
36	1.15	1.17	1.18	1.14	0.02	0.03	−0.01
1′	5.13	5.14	5.15	5.15	0.01	0.02	0.02
2′	–	–	–	–	–	–	–
3′, 4′, 5′	7.39	7.39	7.39	7.39	0.00	0.00	0.00
$O_{XI}H$	2.79	2.95	4.03	3.16	0.16	1.24	0.37
$O_{IV}H$	4.15	5.81	3.80	3.62	1.66	−0.35	−0.53
$O_{X}H$	3.81	4.57	4.36	4.06	0.76	0.55	0.25

$\Delta 1 = \delta_{MON3:Li+} - \delta_{MON3}$, $\Delta 2 = \delta_{MON3:Na+} - \delta_{MON3}$, $\Delta 3 = \delta_{MON3:K+} - \delta_{MON3}$.

2.4. Spectroscopic measurements

The FT-IR spectra of MON3 and its 1:1 complexes (0.07 mol L^{-1}) with $LiClO_4$, $NaClO_4$, and $KClO_4$ were recorded in the mid-infrared region in acetonitrile solutions using a Bruker IFS 113v spectrometer.

A cell with Si windows and wedge-shaped layers was used to avoid interferences (mean layer thickness 170 μm). The spectra were taken with an IFS 113v FT-IR spectrophotometer (Bruker, Karlsruhe) equipped with a DTGS detector; resolution 2 cm^{-1}, NSS = 125. The Happ–Genzel apodization function was used.

All manipulations with the substances were performed in a carefully dried and CO_2-free glove box.

The NMR spectra of MON3 and its 1:1 complexes (0.07 mol L^{-1}) with $LiClO_4$, $NaClO_4$ and $KClO_4$ were recorded in CD_3CN solutions using a Varian Gemini 300 MHz spectrometer. All spectra were locked to deuterium resonance of CD_3CN.

The ^1H NMR measurements in CD_3CN were carried out at the operating frequency 300.075 MHz; flip angle, pw = 45°; spectral width, sw = 4500 Hz; acquisition time, at = 2.0 s; relaxation delay, $d_1 = 1.0$ s; $T = 293.0$ K and using TMS as the internal standard. No window function or zero filling was used. Digital resolution was 0.2 Hz per point. The error of chemical shift value was 0.01 ppm.

^{13}C NMR spectra were recorded at the operating frequency 75.454 MHz; pw = 60°; sw = 19,000 Hz; at =

Table 3
^{13}C NMR chemical shifts (ppm) of MON3 and its complexes in CD_3CN

No. atom	Chemical shift (ppm)				Differences (Δ) between chemical shifts (ppm)		
	MON3	MON3:Li^+	MON3:Na^+	MON3:K^+	Δ1	Δ2	Δ3
1	175.91	176.15	176.79	176.19	0.24	0.88	0.28
2	41.54	41.62	41.74	41.68	0.08	0.20	0.14
3	82.24	82.53	81.91	82.71	0.29	−0.33	0.47
4	37.87	37.45	37.76	38.16	−0.42	−0.11	0.29
5	68.60	69.17	68.76	68.16	0.57	0.16	−0.44
6	37.07	37.45	37.16	37.62	0.38	0.09	0.55
7	71.96	70.06	70.74	70.96	−1.90	−1.22	−1.00
8	35.11	34.17	34.59	34.45	−0.94	−0.52	−0.66
9	108.56	107.99	108.32	108.05	−0.57	−0.24	−0.51
10	39.78	39.61	39.84	39.88	−0.17	0.06	0.10
11	32.60	32.07	33.35	33.92	−0.53	0.75	1.32
12	87.00	87.03	86.63	86.43	0.03	−0.37	−0.57
13	84.48	82.51	82.21	83.58	−1.97	−2.27	−0.90
14	28.45	27.53	27.24	28.21	−0.92	−1.21	−0.24
15	32.06	32.07	30.70	32.00	0.01	−1.36	−0.06
16	88.15	87.92	86.72	86.82	−0.23	−1.43	−1.33
17	86.49	84.91	85.44	85.31	−1.58	−1.05	−1.18
18	35.96	34.03	35.01	35.56	−1.93	−0.95	−0.40
19	34.85	33.71	33.77	33.35	−1.14	−1.08	−1.50
20	77.99	79.44	76.89	77.98	1.45	−1.10	−0.01
21	77.42	74.58	75.60	76.11	−2.84	−1.82	−1.31
22	34.02	33.25	32.17	33.13	−0.77	−1.85	−0.89
23	37.67	36.37	35.75	36.88	−1.30	−1.92	−0.79
24	34.71	34.53	36.22	35.56	−0.18	1.51	0.85
25	97.94	99.63	98.79	98.67	1.69	0.85	0.73
26	67.46	66.40	67.07	67.02	−1.06	−0.39	−0.44
27	16.46	15.97	16.12	16.53	−0.49	−0.34	0.07
28	17.83	17.39	16.66	17.45	−0.44	−1.17	−0.38
29	16.15	16.28	14.40	15.96	0.13	−1.75	−0.19
30	30.14	30.13	30.16	30.39	−0.01	0.02	0.25
31	8.29	8.41	8.11	8.47	0.12	−0.18	0.18
32	26.34	28.50	28.28	28.21	2.16	1.94	1.87
33	11.28	10.85	10.92	11.02	−0.43	−0.36	−0.26
34	12.50	13.13	13.20	12.78	0.63	0.70	0.28
35	58.46	58.71	58.81	58.75	0.25	0.35	0.29
36	12.25	11.28	12.15	11.68	−0.97	−0.10	−0.57
1′	66.96	67.09	67.23	67.06	0.13	0.27	0.10
2′	137.41	137.31	137.21	137.30	−0.10	−0.20	−0.11
3′	128.95	129.04	129.05	129.01	0.09	0.10	0.06
4′	129.40	129.44	129.44	129.42	0.04	0.04	0.02
5′	129.02	129.06	129.09	129.07	0.04	0.07	0.05

$\Delta 1 = \delta_{MON3:Li+} - \delta_{MON3}$, $\Delta 2 = \delta_{MON3:Na+} - \delta_{MON3}$, $\Delta 3 = \delta_{MON3:K+} - \delta_{MON3}$.

1.8 s; $d_1 = 1.0$ s; $T = 293.0$ K and TMS as the internal standard. Line broadening parameters were 0.5 or 1 Hz. The error of chemical shift value was 0.01 ppm.

The ^{1}H and ^{13}C NMR signals were assigned independently for each species using one- or two-dimensional (COSY, HETCOR) spectra.

2.5. PM5 calculations

PM5 semiempirical calculations were performed using the WinMopac 2003 program [27]. In all cases full geometry optimisation of MON3 and its complexes was carried out without any symmetry constraints [28,29].

2.6. Elementary analysis

The elementary analysis was carried out on Perkin-Elmer CHN 240.

3. Results and discussion

The structure of MON3 together with the atom numbering is shown in Scheme 1.

3.1. Electrospray mass spectrometry measurements

The main *m*/*z* peaks observed in the ESI mass spectra of MON3 with the Li$^+$, Na$^+$ and K$^+$ cations used separately at various cone voltage values are summarized in Table 1. Exemplary ESI mass spectra of the 1:1 complex of MON3 with Na$^+$ cation measured at various cone voltages are shown in Fig. 1. According to the data from Table 1, MON3 forms only 1:1 complexes with the cations studied which are very stable up to cv = 70 V. With increasing cone voltage the fragmentation of the respective complexes occurs. The proposed pathways of the fragmentation are shown in Scheme 2. As follows from the *m*/*z* peaks in Table 1 and Scheme 2, the first step of the fragmentation is always the loss of one water molecule as a result of the abstraction of the $O_{IV}H$ or O_XH hydroxyl groups yielding the B or H cations, respectively. Further fragmentation of cation B, in the case of the complexes of MON3 with Li$^+$ and Na$^+$ cations, is realized in two directions with the formation of other types of complexes (C, D, E, F and finally G). Cation C is formed from cation B by the abstraction of the second water molecule. The formation of the D and E fragmentary complexes occurs by the abstraction of the part of the molecule including ester group. Cations F and G can be formed from cations D and E by the loss of one C_3H_4 group. Additionally cation G can be formed by the abstraction of one water molecule from cation F. For the complex of MON3 with K$^+$ cation no abstraction of the part of the molecule including ester group was detected.

The ESI spectrum of the 1:1:1:3 mixture of Li$^+$, Na$^+$, K$^+$ cations and MON3 measured at cv = 30 V is shown in Fig. 2. This figure shows only three characteristic signals at *m*/*z* = 768, *m*/*z* = 784 and *m*/*z* = 800 assigned to the 1:1 complexes of MON3 with Li$^+$, Na$^+$ and K$^+$ cations, respectively. The intensity of the MON3–Na$^+$ complex signal is dominant indicating clearly that MON3 preferentially forms complexes with Na$^+$ cations. The intensity of the signals of the MON3–Li$^+$ and MON3–K$^+$ complexes is

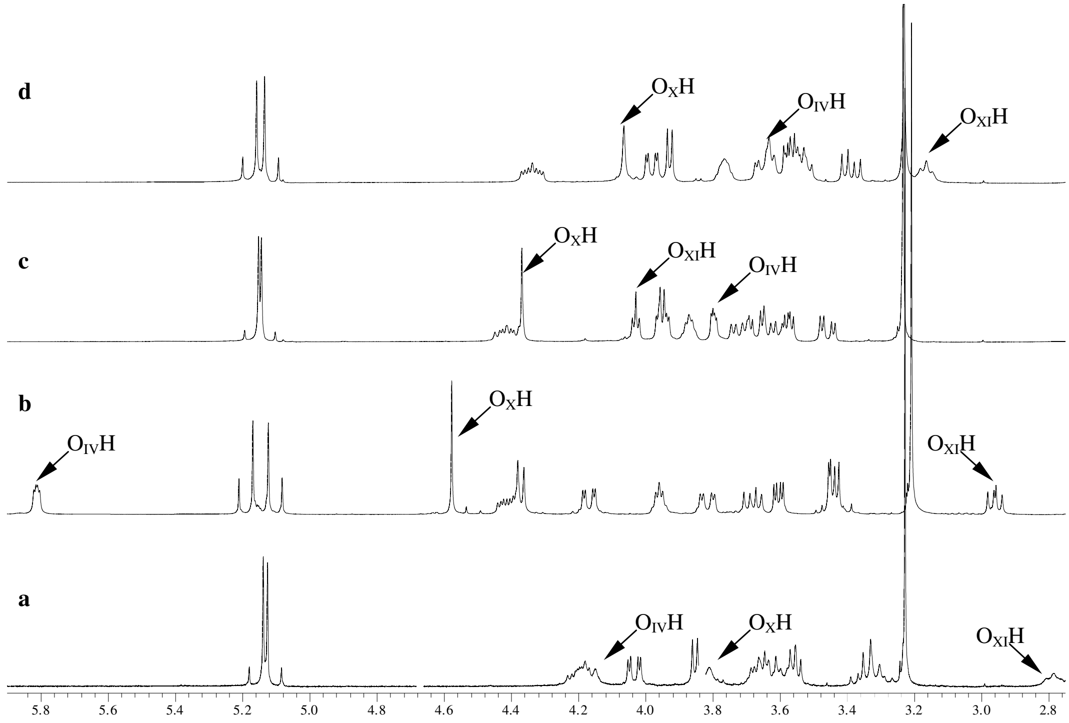

Fig. 3. ^{1}H NMR in region of OH proton signals of: (a) MON3, (b) MON3–Li$^+$, (c) MON3–Na$^+$, and (d) MON3–K$^+$.

significantly lower and comparable demonstrating that MON3 shows only low affinity to Li^+ and K^+ cations.

3.2. ^1H and ^{13}C NMR measurements

The ^1H and ^{13}C NMR data of MON3 in CD_3CN and its 1:1 complexes with Li^+, Na^+ and K^+ cations all in CD_3CN are collected in Tables 2 and 3, respectively. Unfortunately, in contrast to these complexes, the respective MON3 complexes with $RbClO_4$ and $CsClO_4$ are almost insoluble in acetonitrile. The ^1H and ^{13}C signals were assigned independently using one- and two-dimensional (COSY, HETCOR) spectra as well as by the addition of CD_3OD to the probe.

In the ^1H NMR spectra of MON3 and its 1:1 complexes with Li^+, Na^+ and K^+ cations (Table 2), the signals of protons of OH groups are separated. The chemical shift of these signals is strongly dependent on the kind of the cation complexed and this fact is very well illustrated in Fig. 3. In the spectrum of MON3 the OH proton signals observed at 2.79, 3.81, and 4.15 ppm are assigned to $O_{XI}H$, O_XH and $O_{IV}H$ groups, respectively. In the spectra of complexes of MON3 with the Li^+, Na^+ and K^+ cations these signals are shifted in different directions depending on the kind of the cation. This demonstrates that depending on the cation, the respective hydroxyl groups form different intramolecular hydrogen bonds characteristic of different structures of the respective complexes. The conclusion about the different structures can also be deduced from the signal of the protons of the methylene benzyl group (1′) which arise as a doublet of doublets due to the spin–spin geminal couplings. The appearance of such couplings indicates the location of both protons in different fields and formation of typical AB spin–spin coupling structure.

Fig. 3 shows that the most significantly shifted signal of the proton from hydroxyl groups is found in the spectrum of MON3 with Li^+ cation at about 5.81 ppm. This signal is assigned to the $O_{IV}H$ proton, which is involved in the strongest intramolecular hydrogen bond in comparison with all other hydroxyl groups. It is interesting to note that in the spectra of MON3 complexes with Na^+ and K^+ cations, the signals of the $O_{IV}H$ protons are shifted strongly towards lower ppm values demonstrating the weakness of the participation of the $O_{IV}H$ protons in other types of hydrogen bonds due to the formation of different complex structures.

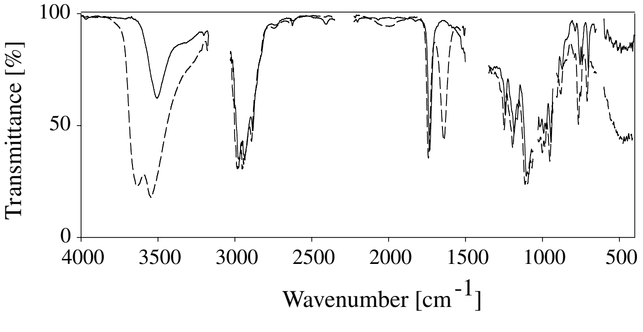

Fig. 4. FT-IR spectra of: water-free MON3 (——) and its 1:3 mixture with water (– –).

A comparison of the ^{13}C NMR chemical shifts in the spectra of complexes with those observed in the spectrum of MON3 suggests not only that the oxygen atoms take part in the cation coordination but also indicates more complex conformation changes evoked by the complexation process. For instance the Δ value of the C_{20} atom for the complex of

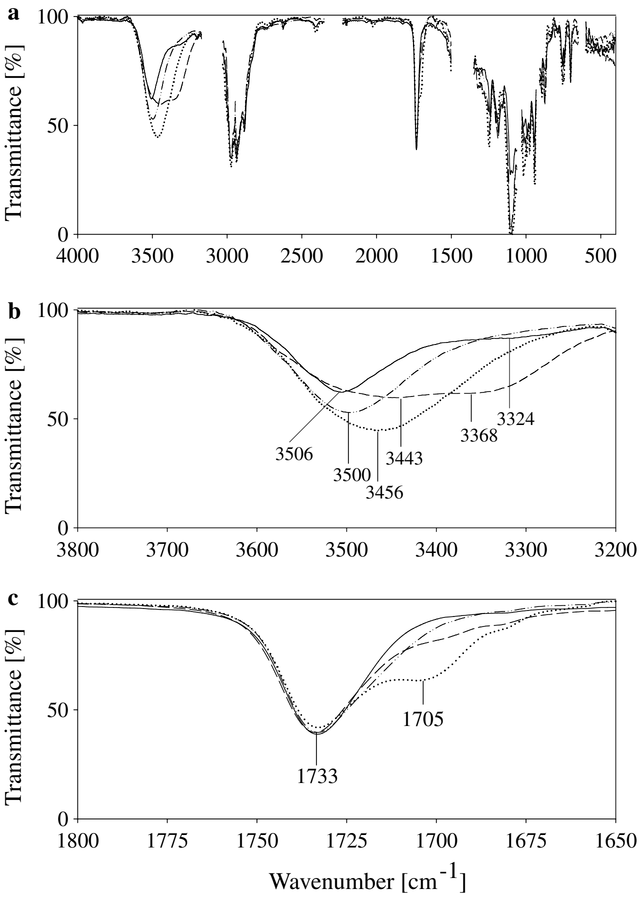

Fig. 5. FT-IR spectra of: (——) MON3, (– –) MON3–Li^+, (···) MON3–Na^+, and (–··–) MON3–K^+ in the ranges of: (a) 4000–400 cm^{-1}; (b) ν(OH) and (c) ν(C=O) stretching vibrations.

Table 4
Heat of formation (kcal mol^{-1}) of MON3 and its complexes with the cations without (A) and with (B) the engagement of carbonyl group in coordination process calculated by PM5 method (WinMopac 2003)

Complex	HOF (kcal mol^{-1})	ΔHOF (kcal mol^{-1})
MON3	−603.11	–
MON3 + $Li^+_{uncomplexed}$(A)	−474.71	−159.18
MON3 + $Li^+_{complexed}$(A)	−633.89	
MON3 + $Li^+_{uncomplexed}$(B)	−474.71	−79.21
MON3 + $Li^+_{complexed}$(B)	−553.92	
MON3 + $Na^+_{uncomplexed}$(A)	−456.58	−240.26
MON3 + $Na^+_{complexed}$(A)	−696.84	
MON3 + $Na^+_{uncomplexed}$(B)	−456.58	−231.02
MON3 + $Na^+_{complexed}$(B)	−687.60	
MON3 + $K^+_{uncomplexed}$(A)	−447.62	−157.77
MON3 + $K^+_{complexed}$(A)	−605.39	
MON3 + $K^+_{uncomplexed}$(B)	−447.62	−48.72
MON3 + $K^+_{complexed}$(B)	−496.34	

$\Delta HOF = HOF_{MON3+Li+complexed} - HOF_{MON3+Li+uncomplexed}$.

MON3 with Li^+ cation is positive, for the complex of MON3 with Na^+ cation it is negative and for the MON3–K^+ complex it is close to zero. This result indicates that the O_{VIII} oxygen atom is involved in the coordination only in the complex of MON3 with Na^+ cation.

3.3. FT-IR studies

In Fig. 4 the FT-IR spectrum of water-free MON3 is compared with the corresponding spectrum of its 1:3 mixture with water, both in acetonitrile solution. This comparison demonstrates that in contrast to the methyl ester of monensin A, MON3 forms no strong bonded hydrates and in consequence also no proton channels.

Most characteristic, in FT-IR spectrum of water-free MON3, are the bands assigned to the ν(OH) vibrations of the O_XH and $O_{XI}H$ groups at 3506 cm^{-1}, and of $O_{IV}H$ group at ca. 3324 cm^{-1} as well as the band assigned to the $\nu(C{=}O)$ vibrations at 1733 cm^{-1}. The spectra of the MON3 complexes with Li^+, Na^+ and K^+ cations are similar to that of MON3 (Fig. 5). According to the NMR data the most significant changes in these spectra

Table 5
The interatomic distances (Å) and partial charges for O atoms of MON3 coordinating metal cations in complex structures calculated by PM5 method (WinMopac 2003)

Complex with monovalent cation	Monovalent cation partial charge	Coordinating atom	Coordinating atom partial charge	Distance (Å) coordinating atom → cation
MON3: Li^+ (A)	+0.462	O_I	–	–
		O_{II}	–	–
		O_{III}	–	–
		O_{IV}–H	−0.384	1.98
		O_V	–	–
		O_{VI}	−0.392	2.14
		O_{VII}	−0.378	2.04
		O_{VIII}	–	–
		O_{IX}	−0.389	2.08
		O_X	–	–
		O_{XI}	–	–
MON3: Na^+ (A)	+0.307	O_I	–	–
		O_{II}	–	–
		O_{III}	–	–
		O_{IV}–H	−0.405	2.28
		O_V	–	–
		O_{VI}	−0.407	2.29
		O_{VII}	−0.399	2.23
		O_{VIII}	−0.401	2.25
		O_{IX}	−0.411	2.30
		O_X	–	–
		O_{XI}	−0.399	2.24
MON3: Na^+ (B)	+0.311	O_I	–	–
		O_{II}	−0.504	2.31
		O_{III}	–	–
		O_{IV}–H	−0.409	2.31
		O_V	–	–
		O_{VI}	−0.410	2.32
		O_{VII}	−0.409	2.31
		O_{VIII}	−0.407	2.29
		O_{IX}	−0.409	2.30
		O_X	–	–
		O_{XI}	−0.406	2.27
MON3: K^+ (A)	+0.483	O_I	–	–
		O_{II}	–	–
		O_{III}	–	–
		O_{IV}–H	−0.422	2.79
		O_V	−0.423	2.80
		O_{VI}	−0.412	2.64
		O_{VII}	−0.430	2.85
		O_{VIII}	–	–
		O_{IX}	−0.428	2.83
		O_X	–	–
		O_{XI}	−0.419	2.73

(A) Structure of MON3 complex in which the $C_1{=}O$ group is not involved in coordination of metal cation; (B) structure of MON3 complex in which the $C_1{=}O$ group is involved in coordination of metal cation.

should be observed in the regions of the ν(OH) and ν(C═O) stretching vibrations. In the spectrum of the MON3–Li^+ complex a broad band in the region 3550–3250 cm^{-1} is observed indicating the involvement of all OH groups in slightly stronger intramolecular hydrogen bonds relative to those of the structure of MON3. This observation is consistent with the ^1H NMR data (Table 2 and Fig. 3). In the spectrum of the MON3–Na^+ complex only one broad band with a maximum at ca. 3456 cm^{-1} is observed, which demonstrates that the hydrogen bonds formed by the O_XH and $O_{XI}H$ groups become slightly stronger and that of $O_{IV}H$ hydroxyl group slightly weaker. In the spectrum of the MON3–K^+ complex also only one band with maximum at 3500 cm^{-1} is observed indicating the weakening of the hydrogen bond of $O_{IV}H$ hydroxyl group within the structure of this complex. This observation is also in full agreement with the ^1H NMR data.

The position of the band assigned to the ν(C═O) vibrations at 1733 cm^{-1}, both in the spectra of MON3 and its complexes with monovalent metal cations, is almost unchanged (Fig. 5c). This fact demonstrates that the oxygen atoms from the C═O ester groups are not engaged in the complexation process of the cations.

The position of the band assigned to the ν(C═O) vibrations at 1733 cm^{-1}, in the spectra of MON3 and its complexes with Li^+ and K^+ cations, is almost unchanged (Fig. 5b). This fact demonstrates that the oxygen atom from the C═O ester group is not engaged in the

Table 6
The length (Å) and angle (°) of the hydrogen bond for MON3 complexes calculated by PM5 method (WinMopac 2003)

Compound	O-atom	Hydrogen bond length (Å) [hydrogen bond angle (°)]		
		$O_{IV}H$	O_XH	$O_{XI}H$
MON3	O_{II}	–	2.89[132.5]	2.95[133.6]
	O_{IX}	2.68[157.2]	–	–
MON3:Li^+ (A)	O_{III}	–	2.73[154.2]	
	O_I	–	–	2.65[143.6]
	O_{IX}	2.45[127.1]	–	–
MON3:Na^+ (A)	O_{IV}	–	2.67[148.1]	–
	O_{III}	–	–	2.59[158.9]
MON3:Na^+ (B)	O_I	–	2.52[133.1]	–
	O_{III}	–	–	2.76[152.9]
MON3:K^+ (A)	O_I	–	2.56[123.1]	–
	O_{III}	–	–	2.55[123.8]

(A) Structure of MON3 complex in which the C_1═O group is not involved in coordination of metal cation; (B) structure of MON3 complex in which the C_1═O group is involved in coordination of metal cation.

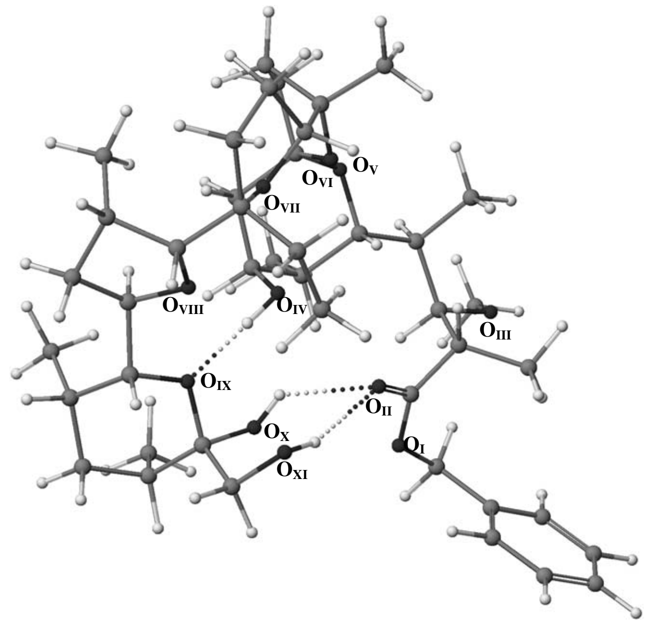

Scheme 3. The structure of MON3 calculated by PM5 method (WinMopac 2003).

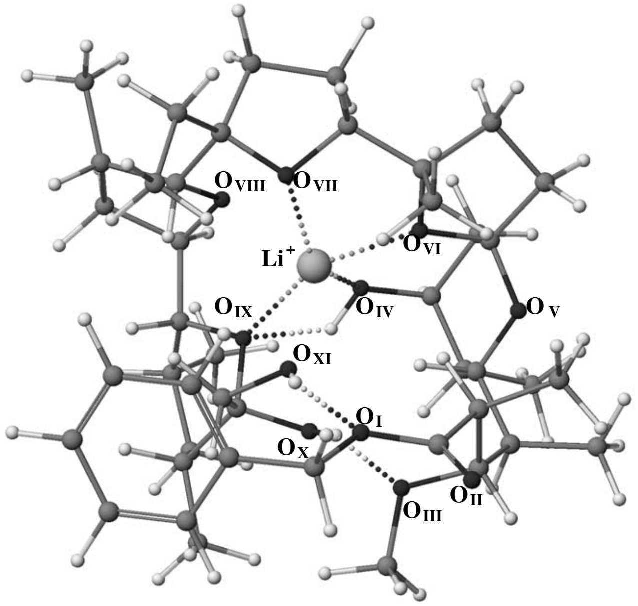

Scheme 4. The structure of MON3–Li^+ complex calculated by PM5 method (WinMopac 2003).

complexation process of these cations. In contrast to this spectrum, the one of MON3 with Na^+ cation shows, besides the band at ca. 1733 cm^{-1} a new band at 1705 cm^{-1}, assigned to the ν(C=O) vibrations of the carbonyl groups interacting with the Na^+ cations. The intensity of this new band is significantly weaker than that at 1733 cm^{-1} indicating that such a structure is not dominant.

3.4. PM5 calculations

Taking into account the experimental findings, the heats of formation (HOF) of the structures of MON3 and its complexes with Li^+, Na^+ and K^+ cations were calculated and collected in Table 4. As follows from the results, the most stable complexes in the gas phase (under the experimental conditions similar to those of ESI measurements) are formed with $Na^+ \gg Li^+ \approx K^+$ cations. This result is in good agreement with the ESI data discussed above. The ΔHOF values show that the structures in which the carbonyl group is involved in the complexation process are energetically less favourable than those in which the carbonyl group is not involved in the complexation process. Only for the MON3–Na^+ complexes the ΔHOF values are of comparable order and this result is in good agreement with the ESI data and with the FT-IR observations.

The interatomic distances between the oxygen atoms of MON3 and the cations and the partial charges at these atoms are given in Table 5. Analysis of these values shows that some oxygen atoms such as O_{IV}, O_{VI}, O_{VII} and O_{IX} are always involved in coordination, irrespective of the kind of the cation, whereas the O_I, O_{II} and O_{III} play no role in this coordination process within the structures of A type, which is in agreement with the ^{13}C NMR data. If the O_{II} oxygen atom from the carbonyl group participates in the coordination of the cation, B type structure in the MON3–Na^+ complex, the calculated coordination distance is slightly longer than those in the A type structure. This result is especially well consistent with the FT-IR data of this complex.

Other oxygen atoms can be involved in the coordination process depending on the type of cation. The coordination distances and the number of coordinating oxygen atoms suggest that all the cations studied can undergo fast fluctuations within the structures of the complexes as it was demonstrated in the complexes of crown ethers with monovalent cations [30].

The lengths and angles of the hydrogen bonds in which the OH groups are engaged are collected in Table 6. The calculated structure of the MON3 indicates that O_{II} oxygen atom from the C=O ester group is engaged in the bifurcated intramolecular hydrogen bonds with two O_XH and $O_{XI}H$ hydroxyl groups (Scheme 3). With the formation of MON3 complexes with cations these hydrogen bonds

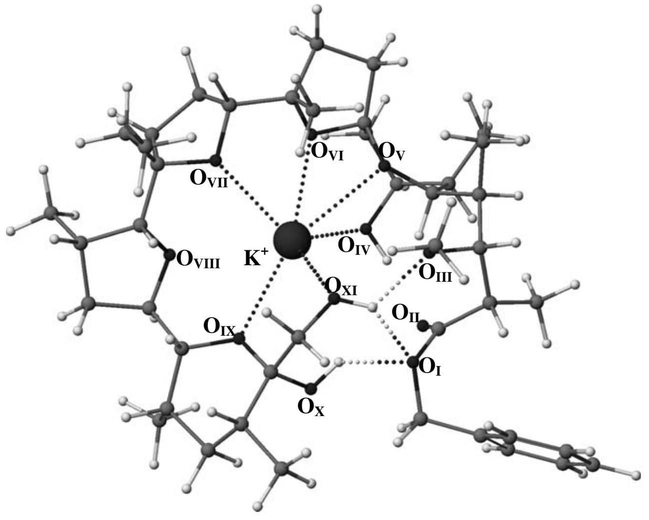

Scheme 6. The structure of MON3–K^+ complex calculated by PM5 method (WinMopac 2003).

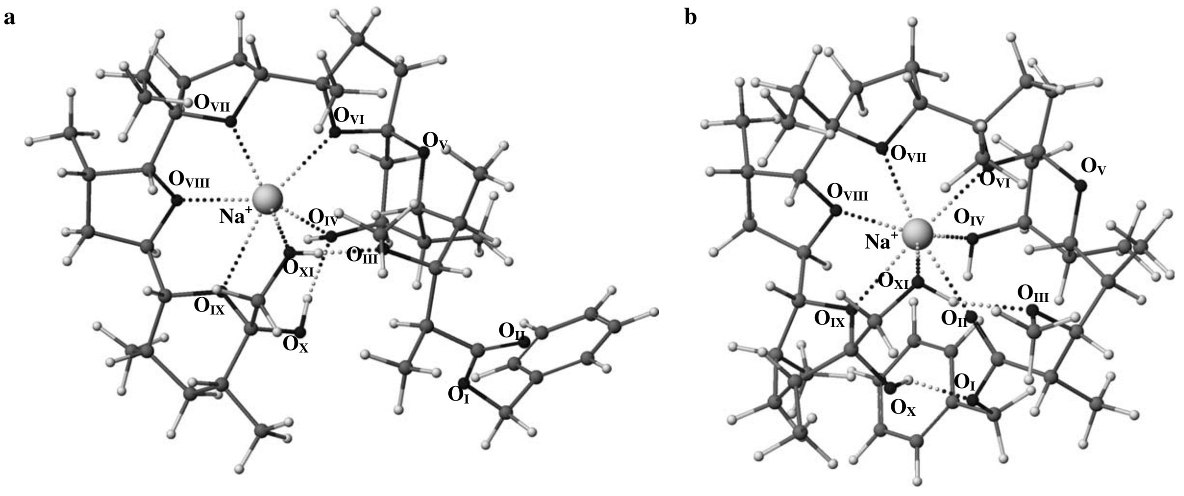

Scheme 5. The structures of two types of MON3–Na^+ complexes: (a) without the engagement of the C_1=O carbonyl group in coordination of the cation – type A, (b) with the engagement of the C_1=O carbonyl group in coordination of the cation – type B calculated by PM5 method (WinMopac 2003).

are always broken. For this reason the ^{13}C NMR signals of the C_1 carbon atoms are shifted toward higher ppm values (Table 3).

In all the calculated structures the $O_{IV}H\cdots O_{IX}$ intramolecular hydrogen bond in the MON3–Li^+ complex was the strongest.

The calculated structures of the MON3 and its complexes with the cations studied are visualized in Schemes 3–6. The hydrogen bonds and the coordination bonds are marked by dots. A comparison of all the calculated structures indicates that only for the MON3 complex with Na^+ cation the molecule forms a pseudo-crown ether structure and therefore, the affinity of MON3 to Na^+ cation is higher than that to the other cations.

References

[1] V.C. Langston, F. Galey, R. Lovell, W.B. Buck, Vet. Med. 80 (1985) 75–84.
[2] Y. Miyazaki, M. Shibuya, M. Sugasawa, O. Kawaguchi, C. Hirose, J. Nagatsu, S. Esumi, J. Antibiot. 27 (1974) 814.
[3] B.C. Granzin, G.McL. Dryden, Anim. Feed Sci. Technol. 120 (2005) 116.
[4] V. Rada, M. Marounek, Ann. Zeotech. 45 (1996) 283.
[5] B. Kohler, H. Karch, H. Schmidt, Microbiology 146 (2000) 1085.
[6] W.L. Duax, G.D. Smith, P.D. Strong, J. Am. Chem. Soc. 102 (1980) 6725.
[7] D.L. Ward, K.T. Wei, J.C. Hoogerheide, A.I. Popov, Acta Crystallogr. Sect. B 34 (1978) 110.
[8] M. Pinkerton, L.K. Steinrauf, J. Mol. Biol. 49 (1970) 533.
[9] W. Pangborn, W. Duax, D. Langs, J. Am. Chem. Soc. 109 (1987) 2163.
[10] P.Y. Barrans, M. Alleume, G. Jeminet, Acta Crystallogr. Sect. B 38 (1982) 1144.
[11] F.A. Almeida Paz, P.J. Gates, S. Fowler, A. Gallimore, B. Harvey, N.P. Lopes, C.B.W. Stark, J. Staunton, J. Klinowskia, J.B. Spencera, Acta Crystallogr. E 59 (2003) 1050.
[12] D.L. Turner, J. Magn. Reson. Ser. B 108 (1995) 137.
[13] T. Martinek, F.G. Riddell, C. Wilson, C.T. Weller, J. Chem. Soc. Perkin Trans. 2 (2000) 35.
[14] A. Nagastu, R. Tanaka, H. Mizukami, Y. Ogihara, J. Sakakibara, Tetrahedron 57 (2001) 3369.
[15] T.S. Edrington, T.R. Callaway, P.D. Varey, Y.S. Jung, K.M. Bischoff, R.O. Elder, R.C. Anderson, E. Kutter, A.D. Brabban, D.J. Nisbet, J. Appl. Microbiol. 94 (2003) 207.
[16] M. Rochdi, A.M. Delort, J. Guyot, M. Sancelme, S. Gibot, J.G. Gourcy, G. Dauphin, C. Gumila, H. Vial, G. Jeminet, J. Med. Chem. 19 (1996) 588.
[17] A. Iacoangeli, G. Melucci-Vigo, G. Risuleo, Biochimie 82 (2000) 35.
[18] W.H. Park, J.G. Seol, E.S. Kim, W.K. Kang, Y.H. Im, C.W. Jung, B.K. Kim, Y.Y. Lee, Br. J. Hematol. 119 (2002) 400.
[19] W.H. Park, E.S. Kim1, C.W. Jung, B.K. Kim, Y.Y. Lee, Int. J. Oncol. 22 (2003) 377.
[20] R. Ferdani, G.W. Gokel, Encyclopedia of Supramolecular Chemistry: Ionophores, Marcel Dekker, New York, 2004, p. 760.
[21] M.S. Shaik, A. Chatterjee, M. Singh, J. Pharm. Pharmacol. 56 (2004) 899.
[22] J.W. Westley, in: Polyether Antibiotics. Naturally Occurring Acid Ionophores, vol. 1, Marcel Dekker, New York, 1982, p. 1.
[23] W. Westley, in: Polyether Antibiotics. Naturally Occurring Acid Ionophores, vol. 2, Marcel Dekker, New York, 1983, p. 51.
[24] B.C. Pressman, Antibiotics and Their Complexes, Marcel Dekker, New York, 1985, p. 1.
[25] A. Huczyński, P. Przybylski, B. Brzezinski, F. Bartl, J. Mol. Struct. 788 (2006) 176.
[26] A. Huczyński, P. Przybylski, B. Brzezinski, F. Bartl, Biopolymers 81 (2006) 282.
[27] J.J.P. Stewart, J. Comput. Chem. 10 (1989) 209.
[28] J.J.P. Stewart, J. Comput. Chem. 12 (1991) 320.
[29] CAChe 5.04 UserGuide, Fujitsu, 2003.
[30] B. Brzezinski, G. Schroeder, A. Rabold, G. Zundel, J. Phys. Chem. 99 (1995) 8519.